A Thermal Model for Photovoltaic Panels Installed on a Vehicle Body

F. A. Tiano & G. Rizzo
Department of Industrial Engineering
University of Salerno, Fisciano, Italy
E-mail: [ftiano, grizzo] @unisa.it

Topics: Photovoltaics, Hybrid and Electric Vehicles

The integration of photovoltaic panels on electric and hybrid vehicles is gaining interest, due to the exigencies of reducing carbon footprint of road transportation. In order to develop mathematical models for making cost-benefit analysis in designing a solar assisted electric or hybrid vehicle and to achieve real-time optimal management of energy flows, a reliable estimation of the useful energy from PV is needed. In this paper a model able to estimate temperature effects for PV panels installed on a car is developed, and the results of simulation over a route and varying time, speed and panel orientation are presented and discussed.

1 INTRODUCTION AND MOTIVATIONS

Carbon dioxide (CO_2) production from the automotive systems is having a great impact on climate changes and fossil fuel depletion, and, for these reasons, sustainable mobility issues have more attention both from specialist and public opinion: there is the need of reducing CO_2 emissions rapidly to meet the international energy savings requests [1].

The most suitable solution to this problem consists in the increasing use of hybrid electric vehicles (HEV) and battery electric vehicles (BEV). Hybrid electric vehicles can represent an effective way to a more sustainable mobility in the meantime that the several issues preventing a mass diffusion of electric or fuel-cell vehicles (FCEV) will be solved: cost of batteries, recharging time and their impact on electrical grid, and, last but not least, extension of carbon free electric production.

Both HEVs and BEVs are characterized by the presence of a battery of significant capacity, ranging from about 1 kWh in HEVs to more than 20 kWh in BEVs. This battery could in principle be recharged also by photovoltaic panels, located on recharging stations or, also, on the vehicle itself. This latter solution has been used in last decades for the propulsion of solar cars. These vehicles, being powered only by the sun, in spite of some spectacular outcomes in competitions as World Solar Challenge, do not represent a practical alternative to conventional cars, due to limitations on maximum power, range, dimensions, and mainly because of the intermittence of solar source. Photovoltaics can instead represent an effective and clean additional source of energy for both HEVs and BEVs. Indeed, the potential advantages of solar energy are clear: it is free, abundant and rather evenly distributed, but there are also limitations, like intermittency due to the effects of relative motion between Earth and Sun, time variable due to weather conditions and, last but not least, its energy density [1]. The scarce attention and some sort of skepticism about the direct use of solar energy in cars may be explained by the misleading habit to analyze the automotive systems in terms of power, instead of energy [2]. PV panels, when properly designed and used, may allow meeting a significant share of the total energy required by the car, in particular for urban driving [1]. Moreover, their economic feasibility for automotive applications appears more and more encouraging, due to the spectacular reduction in their cost occurred in last decades (Fig. 1).

Moreover, the presence of a photovoltaic panel on a Plug-In Hybrid Electric Vehicle (PHEV) can enhance the development of Vehicle to Grid (V2G) technology: in this approach, the plug-in vehicles, besides receiving power when parked, can also provide

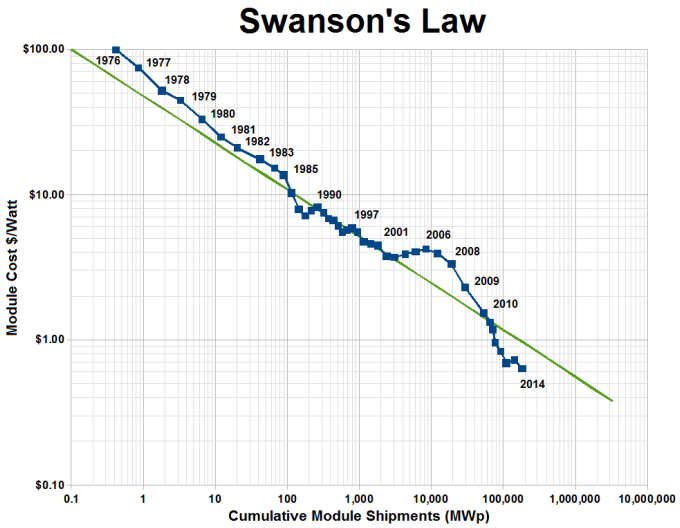

Figure 1: Trends of cost for photovoltaic modules

power to the grid. Use of PHEVs for V2G can provide benefits to both vehicle owner and the power utility company, apart from the reduced tailpipe emissions and increased mileage, particularly when the number of vehicle connected to the grid is large [3].

The available surface for PV on a car is quite limited with respect to stationary applications. It is therefore compulsory to maximize their efficiency and to predict precisely the useful energy output. A quantitative evaluation of solar contribution is needed when making cost-benefit analysis in designing a solar assisted vehicle. Moreover, a prediction of the future incoming energy is also useful to achieve optimal vehicle energy management for battery recharge in BEV and PHEV and for State-of-Charge (SOC) real-time management in hybrid vehicles [4].

In particular, the reduction of the cost and the availability of flexible and semi-transparent modules make it possible to consider installing PV cells not only on the vehicle roof, in almost horizontal position, but also on other parts of car body, as car sides, windows and hood. Estimating the trade-off between costs and benefits for those solutions requires the availability of more complex irradiation models, not limited to the direct irradiation only but including diffuse component too, and the estimation of the temperature effects on PV performance during both parking time and road operation. Our research group is working on both these aspects. The present paper is focused on panel temperature, one of the key parameters affecting solar panel efficiency.

As it is known, a single-junction solar cell absorbs most of the

incident solar irradiance with photon energy above its semiconductor band gap. Therefore, a significant portion of solar energy is converted into heat, which involves heating the cell itself and then give rise to inefficiency and an acceleration to the aging rate. For instance, in a standard commercial crystalline silicon solar cell, every 1 °C increase in temperature leads to an efficiency reduction of the order of 0.45% [5].

This work proposes a model for the evaluation of the temperature of a plane surface exposed to the Sun, considering conductive and forced convective heat exchange, and the relative connection with the photovoltaic module efficiency. The goal is to establish a computational model suitable for estimating the real efficiency of a photovoltaic panel when used in electric or hybrid vehicles, and to validate it with experimental results both in laboratory and on a prototype of solar assisted vehicle.

2 FORMULATION OF THE PROBLEM

The operating temperature of a PV cell has a remarkable influence on its efficiency. Its effect has been investigated by several researchers, producing different models and correlations to describe its effects [6].

Maximum power is usually expressed as a product of voltage and current at the maximum power point. Introducing the fill factor FF, maximum power can be also expressed as a function of open circuit voltage and short circuit current:

$$P_m = V_m I_m = (FF) V_{oc} I_{sc} \tag{1}$$

Both open circuit voltage and fill factor decrease significantly with temperature, while short circuit current exhibit a slight increase [7]. Starting from these assumptions, and with some simplifications, a linear relationship for the efficiency is often used:

$$\eta_c = \eta_{T_{ref}} [1 - \beta_{ref}(T_c - T_{ref}) + \gamma \log I(t)] \tag{2}$$

where $\eta_{T_{ref}}$ is the module's electrical efficiency at the reference temperature, $\eta_{T_{ref}}$, and at solar radiation flux of 1000 W/m^2 [8]. T_c is the cell operating temperature. The temperature coefficient β_{ref} and the solar radiation coefficient γ depend on the material. For crystalline silicon modules they are about equal to 0.004 and 0.12, respectively [9]. The latter term is usually set as zero [10] and Eq. 2 reduces to:

$$\eta_c = \eta_{T_{ref}} [1 - \beta_{ref}(T_c - T_{ref})] \tag{3}$$

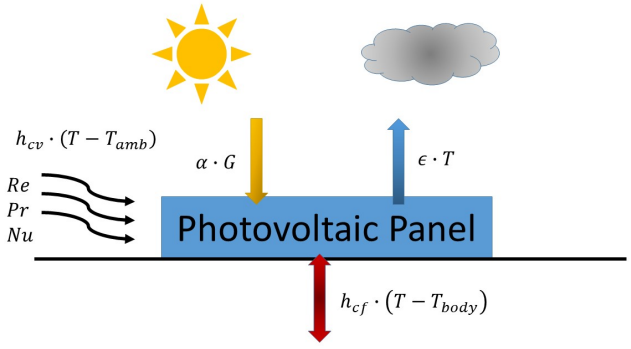

Figure 2: Schematic depiction of the thermal model

In order to estimate the actual efficiency, a mathematical model to determine the temperature of the photovoltaic panel installed on the body of the vehicle has been developed. The photovoltaic panel is modeled as a grey body. The model takes into the account the incident solar radiation, the radiation emitted by the photovoltaic panel and the heat exchange between the panel and the surroundings via convective and conductive heat exchange factors.

Table 1: Photovoltaic module parameters

Panel parameters	SP 52 Q	SP 144
Length $[m]$	0.601	1.490
Width $[m]$	0.546	0.546
Thickness $[m]$	0.002	0.002
Area $[m^2]$	0.328	0.814
Peak power $[W]$	52	144
Ref. efficiency $[\%]$	23	23
Ref. temperature $[°C]$	25	25

2.1 Composition of the panel

The hybrid solar vehicle developed by researchers of the Energy and Propulsion Laboratory of the University of Salerno and of the spin-off company eProInn is equipped with two photovoltaic modules installed on the body of the vehicle. These are both thin-film monocrystalline silicon modules made by Solbian and they are composed of several layers. Two different models are installed on the hood and on the roof of the vehicle: respectively the SP 52 Q (52 W peak power) and the SP 144 (and 144 W peak power).

Both modules have the same structure and are made of nine main layers:

- *Front cover*: The front layer of the module is, actually, composed of three different sub-layers. This consists in the overlap of Ethylene Tretrafluoroethylene Copolymer (ETFE), Polyethylene terephthalate (PET) and Polyethylene (PE) layers.
- *Anti-Reflective Coating (ARC)*: a standard ARC layer is applied on the PV cells in order to channels the protons into the cells.
- *Photovoltaic (PV) Cells*: Monocrystalline silicon cells made by Sunpower are used in Sobian modules.
- *Rear Contact*: Sunpower PV cells come with a Copper rear contact layer.
- *Incapsulating layer*: The PV Cells are incapsulated in a PE layer to provide resistance and electrical isolation.
- *Back layer*: The back layer of the module is made in PET.

PV modules are glued on the the vehicle body. Neglecting the glue layer, the heat exchange of modules has to consider the vehicle body and the underneath insulating (both thermal and acoustic) material. Table 2 contains thickness (t), thermal conductivity ($W/m/K$), density (ρ) and specific heat capacity (c) of each layer of the PV module. From these properties is possible to find the thermal resistance R_{Th} and thermal capacitance C_{Th} of each layer, defined as follows [11]:

$$R_{Th} = \frac{t}{kA_s} \qquad C_{Th} = \rho c A_s t \tag{4}$$

Analogously, the layers of the vehicle body are considered. Table 3 contains the thermal properties and thickness of vehicle body (steel) and insulating material (polyurethane).

2.2 Energy balance equation

For each layer of the PV module and of the vehicle body a thermal energy balance taking into account radiative, convective and conductive heat exchanges with the other layers and the environment is applied.

The general equation of the i-esim layer is the following:

Table 2: Photovoltaic module layers properties. [12, 13]

Layer	Thickness t, (m)	Thermal conductivity k, $(W/m/K)$	Density ρ, (kg/m^3)	Specific heat c, $(J/kg/K)$
1. ETFE	$30 \cdot 10^{-6}$	0.24	1700	1950
2. PET	$300 \cdot 10^{-6}$	0.15	1370	1000
3. PE	$50 \cdot 10^{-6}$	0.49	920	1900
4. PE	$400 \cdot 10^{-6}$	0.49	920	1900
5. ARC	$100 \cdot 10^{-9}$	32	2400	691
6. PV Cells	$140 \cdot 10^{-6}$	148	2330	677
7. Rear contact	$10 \cdot 10^{-6}$	390	8920	385
8. PE	$400 \cdot 10^{-6}$	0.49	920	1900
9. PET	$300 \cdot 10^{-6}$	0.15	1370	1000

Table 3: Vehicle body layers properties. [12]

Layer	Thickness t, (m)	Thermal conductivity k, $(W/m/K)$	Density ρ, (kg/m^3)	Specific heat c, $(J/kg/K)$
Hood	$15 \cdot 10^{-4}$	52	7500	502
Roof	$8 \cdot 10^{-4}$	52	7500	502
Insulating	$15 \cdot 10^{-3}$	0.02	1.2	1500

$$C_{Th,i}\frac{\mathrm{d}T_i}{\mathrm{d}t} = \begin{cases} A_s\ G\ \alpha - P_{PV}(G) \\ A_s\ \varepsilon\ \sigma\ F_{ft-sky}\ (T_i^4 - T_{sky}^4) \\ A_s\ \varepsilon\ \sigma\ F_{ft-ground}\ (T_i^4 - T_{ground}^4) \\ A_s\ h_{cv}\ (T_i - T_{amb}) \\ A_s\ (1/R_{Th})\ \Delta T \end{cases} \tag{5}$$

Front layer of the module has convective and radiative heat exchange with the environment and conductive heat exchange with the underneath layers. Internal layers only have conductive heat exchange. Exception is made for the PV Cells which also is characterized also by a radiative energy flux. The insulating material under the vehicle body has conductive heat exchange with the upper layers and a convective heat exchange with the air in, respectively, in the engine compartment and the cabin.

2.2.1 *Front layer convective heat transfer*

The convective heat exchange factor depends on the relative speed of air in respect of the PV panel. For this application, the speed of air has been set equal to the the speed of the vehicle. Due to the air flux flowing over the surface of the PV panel there is the need to determine both the forced heat transfer coefficient, h_{forced}, and the free convective heat transfer coefficient, h_{free}.

Forced convection plays the major role in the heat exchange of the module. Several previous works on photovoltaic panels have established a direct correlation between the wind speed and the forced convection heat transfer factor through wind tunnel tests [14, 15, 16, 17] and outdoor tests [18, 19, 20].

These works were performed on standard stationary photovoltaic panels. For this study, where the module is installed on a moving vehicle, a classical Nusselt Relations approach is used, which is defined as [11]:

$$\overline{Nu} = \frac{hL}{k_{air}} \tag{6}$$

For the forced convection, the Nusselt number is derived, in turn, from the Reynolds and Prandtl numbers [11]:

$$\begin{aligned} Pr &= \mu_{air}\frac{c_{p,air}}{k_{air}} \\ Re &= \rho_{air}\frac{u_{air}L}{\mu_{air}} \end{aligned} \tag{7}$$

Depending on the value of the Reynolds the air flow is laminar or turbulent, and the Nusselt number is calculated as [13]:

$$\begin{cases} \overline{Nu} = 0.664\ Pr^{1/3}\ Re^{1/2}, & \text{for } Re \leq 1.2 \cdot 10^5 \\ \overline{Nu} = 0.037\ Pr^{1/3}\ Re^{4/5}, & \text{for } Re > 1.2 \cdot 10^5 \end{cases} \tag{8}$$

For the free convection, the Nusselt number is calculated as [21]:

$$\overline{Nu} = 0.21\ (Gr\ Pr)^{0.32} \tag{9}$$

where the Grashof number is defined as [13]

$$Gr = \frac{g\ \cos\beta\ (T_{cell} - T_{amb})\ L^3}{T_{amb}\ \nu^2} \tag{10}$$

The effective convection from the top layer heat exchange factor is a combination of the free and the forced convection [21]:

$$h_{front} = \sqrt[3]{h_{forced}^3 + h_{free}^3} \tag{11}$$

2.2.2 *Back convective heat transfer*

The convective heat transfer factor from the back side of the system (i.e., the insulating material of the vehicle body) is derived, again, from the Nusselt number. Unlike the front layer, for the last layer there is only the free convection. The Nusselt number, in this case, is calculated as [13]:

$$\overline{Nu} = \left[0.825 + \frac{0.387\ (Gr\ Pr)^{1/6}}{\left[1 + (0.492/Pr)^{9/16}\right]^{8/27}}\right]^2 \tag{12}$$

For this study, an underhood temperature equal to 85 °C [22] and a cabin temperature equal to 26 °C have been considered.

2.2.3 *View factors for the radiative heat transfer*

Radiative heat transfer from the PV modules towards the sky and ground have to take into account the view factor of the module due to the fact that they are installed on tilted surfaces.

View factors are calculated as [13]:

$$\begin{aligned} F_{ft-sky} &= \frac{1}{2}\ (1 + \cos\beta) \\ F_{ft-ground} &= \frac{1}{2}\ (1 - \cos\beta) \end{aligned} \tag{13}$$

The ground temperature T_{ground} for the radiative heat transfer is assumed to be equal to the ambient temperature [13]. Instead, the sky temperature is derived from the ambient temperature as [21]:

$$T_{sky} = 0.0552 \cdot T_{amb}^{1.5} \tag{14}$$

2.2.4 *Incoming solar irradiance*

The incoming solar radiation on the photovoltaic is calculated from the Solar Constant ($I_0 = 1367 W/m^2$) and takes into account the angle of incidence between the radiation and the normal to the module surface:

$$I = I_0 \; 1.1 \; 0.7^{AM^{0.678}}$$
$$I_b = I \; \cos\theta \tag{15}$$

2.2.5 *Absorptivity and emissivity*

Absorptivity α and emissivity ε data from [23] have been used in this study. This data are very close to those found in literature. For the monocrystalline silicon photovoltaic module they are, respectively, equal to 0.92 and 0.85.

3 SIMULATIONS

For the simulation of the temperature of the photovoltaic panels installed on the hood and on the roof of the vehicle, a route of the vehicle should be defined. For this study, the road from Pagani (Salerno, Italy) to University of Salerno, with start at 10 A.M., has been considered. Traffic conditions are neglected and it is assumed that the vehicle speed (i.e., the speed of air flowing over the modules) is equal to the speed limits of the roads. The route, shown in Fig. 3, is a mixed urban-motorway 20 km travel and last about 16 minutes.

Figure 3: Route from Pagani to University of Salerno

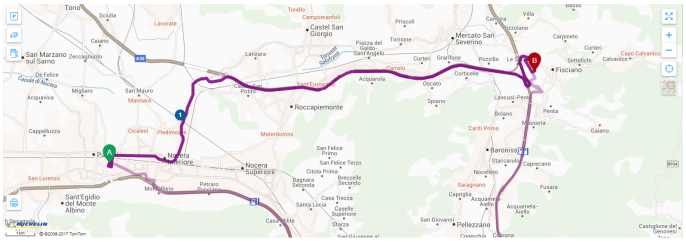

The velocity profile is shown in Fig.4. For the sake of simplicity, it is assumed that air direction is parallel to the direction of the vehicle.

Figure 4: Velocity profile of the vehicle

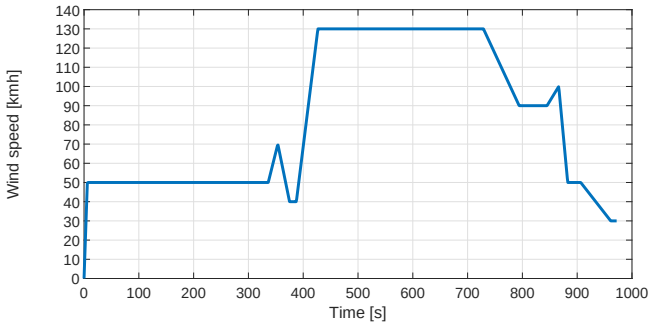

External ambient temperature and the respective sky temperature on the day of the simulation (April 3rd, 2018) is shown in Fig. 5.

Figure 5: Ambient air and sky temperature profile

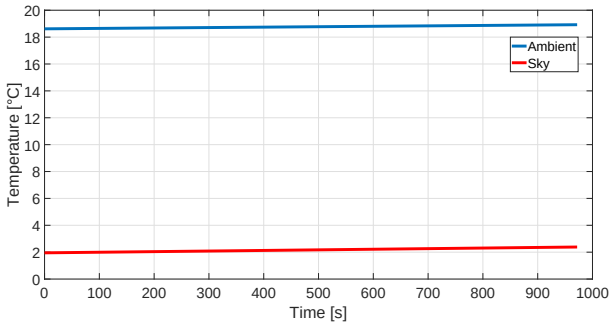

Beam solar radiation both on the roof and the hood of the vehicle are plotted in Fig. 6.

Figure 6: Beam irradiance over roof and hood

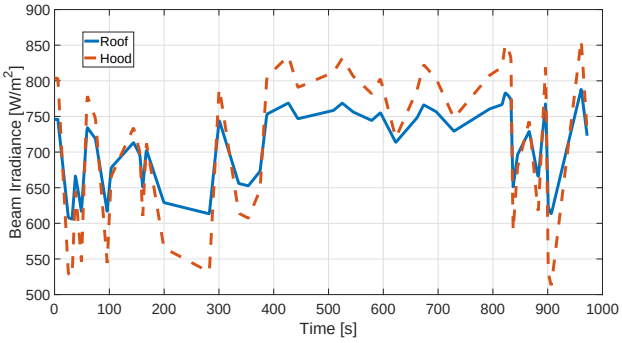

4 RESULTS

Known all the boundary conditions (i.e., wind speed, air and sky temperatures, and solar irradiance), it is possible to estimate the temperature of photovoltaic panels during the travel. It has been assumed that the temperature of the module at the beginning of the simulation ($t = 0$) is equal to ambient temperature.

Fig. 7 show the estimation of the temperature of the PV panel installed on the hood of the vehicle during the travel. As expected, the response of the temperature with the solar irradiance is slower than the variation of the irradiance itself. This is due to the thermal inertia of the system. The speed of the vehicle plays an important role in the panel refrigeration. In fact, when the vehicle drives on the motorway the temperature drops of almost 5 °C, thus compensating the increase of solar irradiance. At the end of the simulation, when the vehicle enters in the urban part of the drive-cycle the temperature increases again reaching almost 35 °C.

Figure 7: Temperature response of hood PV panel with irradiance

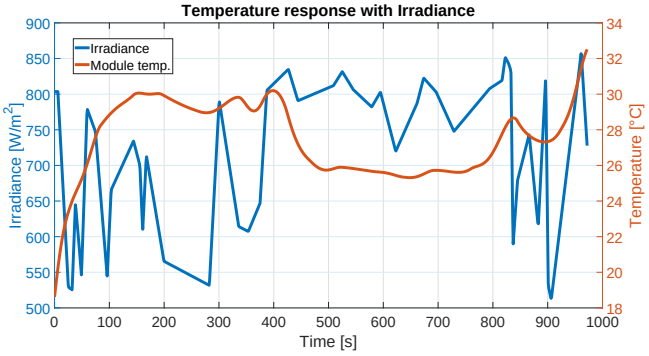

The effect of the temperature on the panel efficiency according

to Eq. 3 is shown in Fig. 8. At the highest temperature reached during the travel, the efficiency of the panel reduces up to 3.9% and of 1.87% on average than the reference one.

Figure 8: Efficiency of the hood PV panel

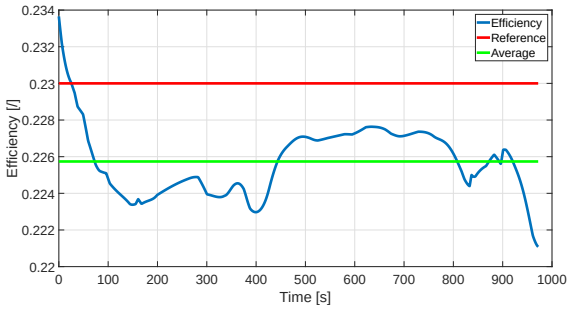

Analogously, Fig. 9-10 show the temperature response with solar irradiance and the efficiency of the PV panel installed on the roof of the vehicle. During the travel, the temperature of the roof of the vehicle is slightly lower than the one of the hood. This can be explained considering that the cabin of the vehicle has a temperature lower than the underhood one, and that the solar irradiance - for that conditions - on the roof is slightly lower than the one on the hood because of the different slope of the two parts of the vehicle (16° to 8°, respectively).

Figure 9: Temperature response of roof PV panel with irradiance

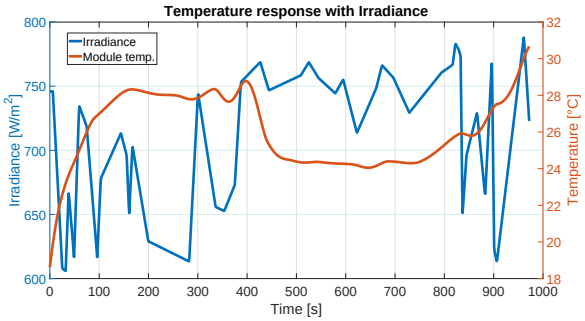

Figure 10: Efficiency of the roof PV panel

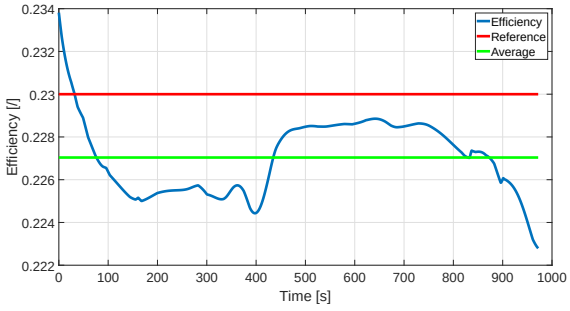

At the end of the simulation, the temperature of the panel on the roof of the vehicle is almost equal to 33 °C. The efficiency of this panel is slightly higher than the other one. Specifically, the reduction than the reference efficiency stops at 3.1% (1.3% on average).

5 CONCLUSIONS

The thermal model presented in this study allows to estimate the temperature of photovoltaic panels installed on the body of a vehicle and to evaluate the efficiency drop of panels themselves. The model incorporates atmospheric condition and the material composition of the photovoltaic panels and of the body of the vehicle. The model can be applied both to BEVs and HEVs.

Estimation of temperatures and efficiency of two thin-film monocrystalline silicon photovoltaic panels installed on the hood and on the roof of a prototype realized by research of University of Salerno and of eProInn have been made. The model has been used to performed the estimation with the vehicle traveling on a mixed urban-motorway route, but it can be also used during parking time if wind speed data are available.

It must be considered that, as long as the vehicle is moving, the air flowing on the panel installed on the hood of the vehicle lowers its temperature. But once arrived at destination, the contribution of forced convection heat transfer reduces. In case of HEVs, the photovoltaic panel installed on the hood is dangerously exposed to an increase of temperature since the engine compartment under the hood will keep its temperature high until the engine naturally chills. This will not only reduce the efficiency of the panel for stationary generation of electricity, but even damage the panel itself in the long period.

Consequently, the use of photovoltaic panels in HEV applications should let to consider an alternative design of the insulation material usually installed on the back of the hood in order to prevent damages to the panels.

The model developed in this study can be further improved by including the thermal simulation of the cabin during parking periods. In fact, in this condition the temperature of the PV modules can attain quite high values (e.g., 50 °C) thus reducing significantly the module efficiency.

ACKNOWLEDGMENTS

This study is supported by a grant from European Union (LIFE-SAVE Solar Aided Vehicle Electrification LIFE16 ENV/IT/000442) and by European Funds for the OPTimised Energy Management and USe (OPTEMUS) Project.

LIST OF SYMBOLS

Latin symbols	
c	Specific heat, $J/kg/K$
d	Panel length, m
h	Heat exchange coefficient, $W/m^2/K$
k	Thermal conductivity, $W/m/K$
t	Thickness, m
u	Air relative speed, m/s
A	Surface, m^2
C	Thermal capacitance, J/K
F	View Factor, /
FF	Fill factor, /
G	Solar flux, W/m^2
Gr	Grashof number, /
I	Current, A
Nu	Nusselt number, /
P	Power, W
Pr	Prandtl number, /
R	Thermal resistance, K/W
Re	Reynolds number, /
T	Temperature, K
V	Voltage, V
Greek symbols	
α	Absorption factor, /
β	Panel slope, °
γ	Solar radiation coefficient, m^2/W
ε	Emission factor, /
θ	Angle of incidence, °
μ	Viscosity, $Pa\ s$
ρ	Density, kg/m^3
σ	Stefan-Boltzmann constant

Subscripts	
amb	Ambient air
body	Vehicle body
c	Photovoltaic cell
cd	Conductive
cv	Convective
ft	Front
ground	Ground
m	Maximum
oc	Open-circuit
ref	Reference
sc	Short-circuit
sky	Sky
Th	Thermal
Superscripts	
AM	Air Mass, /

REFERENCES

[1] G. Rizzo. Automotive applications of solar energy. *IFAC Proceedings Volumes*, 43(7):174 – 185, 2010. 6th IFAC Symposium on Advances in Automotive Control.

[2] G. Rizzo, I. Arsie, and M. Sorrentino. Hybrid solar vehicles. In Reccab Manyala, editor, *Solar Collectors and Panels, Theory and Applications*, chapter 4, pages 79–96. Sciyo, 2010.

[3] Willett Kempton, Jasna Tomic, Steven Letendre, Alec Brooks, and Timothy Lipman. Vehicle-to-grid power: Battery, hybrid, and fuel cell vehicles as resources for distributed electric power in california. Institute of transportation studies, working paper series, Institute of Transportation Studies, UC Davis, 2001.

[4] G. Rizzo and M. Sorrentino. Introducing sunshine forecast to improve on-board energy management of hybrid solar vehicles. *IFAC Proceedings Volumes*, 43(7):276 – 281, 2010. 6th IFAC Symposium on Advances in Automotive Control.

[5] Wei Li, Yu Shi, Kaifeng Chen, Linxiao Zhu, and Shanhui Fan. A comprehensive photonic approach for solar cell cooling. *ACS Photonics*, 4(4):774–782, 2017.

[6] E. Skoplaki and J.A. Palyvos. On the temperature dependence of photovoltaic module electrical performance: A review of efficiency/power correlations. *Solar Energy*, 83(5):614 – 624, 2009.

[7] H.A. Zondag. Flat-plate pv-thermal collectors and systems: A review. *Renewable and Sustainable Energy Reviews*, 12(4):891 – 959, 2008.

[8] D.L. Evans. Simplified method for predicting photovoltaic array output. *Solar Energy*, 27(6):555 – 560, 1981.

[9] Swapnil Dubey, Jatin Narotam Sarvaiya, and Bharath Seshadri. Temperature dependent photovoltaic (pv) efficiency and its effect on pv production in the world a review. *Energy Procedia*, 33(Supplement C):311 – 321, 2013. PV Asia Pacific Conference 2012.

[10] D.L. Evans. Simplified method for predicting photovoltaic array output. *Solar Energy*, 27(6):555 – 560, 1981.

[11] Frank P. Incropera. *Fundamentals of Heat and Mass Transfer*. John Wiley & Sons, Inc., USA, 2006.

[12] Goodfellow. Materials database. `http://www.goodfellow.com`.

[13] S. Armstrong and W.G. Hurley. A thermal model for photovoltaic panels under varying atmospheric conditions. *Applied Thermal Engineering*, 30(11):1488 – 1495, 2010.

[14] William H. McAdams. *Heat transmission [by] William H. McAdams*. McGraw-Hill New York, 3d ed. edition, 1954.

[15] J. H. Watmuff, W. W. S. Charters, and D. Proctor. Solar and wind induced external coefficients - Solar collectors. Technical report, June 1977.

[16] Peter J Lunde. *Solar thermal engineering : space heating and hot water systems*. New York : Wiley, 1980. ISBN: 0471030856.

[17] E. M. Sparrow, J. W. Ramsey, and E. A. Mass. Effect of finite width on heat transfer and fluid flow about an inclined rectangular plate. *Journal of Heat Transfer*, 101(2):199–204, 5 1979.

[18] R. C. Lessmann. Heat transfer during wind flow over rectangular bodies in the natural environment. *Journal of Heat Transfer*, 103(2):262–267, 5 1981.

[19] R.J. Cole and N.S. Sturrock. The convective heat exchange at the external surface of buildings. *Building and Environment*, 12(4):207 – 214, 1977.

[20] S. Sharples and P.S. Charlesworth. Full-scale measurements of wind-induced convective heat transfer from a roof-mounted flat plate solar collector. *Solar Energy*, 62(2):69 – 77, 1998.

[21] M.K. Fuentes. A simplified thermal model for flat-plate photovoltaic arrays. Technical report, U.S. Department of Energy Office of Scientific and Technical Information, United States, 5 1987.

[22] Mahmoud Khaled, Fabien Harambat, and Hassan Peerhossaini. Underhood thermal management: Temperature and heat flux measurements and physical analysis. *Applied Thermal Engineering*, 30(6):590 – 598, 2010.

[23] Mikhail N. Polyanskiy. Refractive index database. `https://refractiveindex.info`.